Sohag Journal of Sciences
*An International Journal*

# Comparison between the Charge- discharge processes of Zn-In and Zn-Sb alloys in an alkaline medium for batteries application

*Hoda A. El –Shafy Shilkamy*[1*], *Mahmoud Elrouby*[1,2*], *Hossnia S. Mohran*[1], *A. Elsayed*[1]

[1] Department of Chemistry, Faculty of Science, Sohag University, Sohag, Egypt. 82524
[2] Faculty of Science, King Salman International University, Ras sudr, Sinai, 46612, Egypt.

Received: 24 Apr. 2022, Revised: 22 May 2022, Accepted: 7 Jun. 2022.
Published online: 1 Spt. 2022

**Abstract:** In alkaline batteries, zinc is one of the most commonly used and significant metals. It has been discovered that adding a small amount of indium or antimony as an alloying element to zinc enhances battery longevity while maintaining zinc's sacrificial protection. Electrochemically examined using Galvanostatic Charge Discharge techniques, charge-discharge performance for Zn, Zn-1% In, and Zn-1% Sb alloys in 6 M KOH solution. According to the charge-discharge data, introducing 1 percent Into Zn, the observable voltage is moved to a higher negative potential value. However, by adding the same quantity of Sb, this voltage is switched to a less negative direction. In comparison to Sb, however, greater capacitance values can be attained at 1% In. This suggests that 1% In alloying with Zn has a greater favorable impact on charge effectiveness and capacitance than 1% Sb alloying. Zn-1%In alloy has a high capacitance value (179 F\g), whereas Zn and Zn-1%Sb alloy have capacitance values of 174 and 162 F\g, respectively. Furthermore, compared to Zn-1 percent Sb alloy, the discharge duration of Zn-1 percent In alloy is longer. Finally, modest alloying of In or Sb with Zn can be considered viable composites for long-life alkaline.

**Keywords**: Batteries application, Alkaline solution, Zn-In bimetallic, Zn-Sb alloy, Charge-discharge processes.

## 1 Introduction

Rechargeable batteries (secondary batteries) are vital in today's technology. In general, by substituting some active material with conductive fillers and wider pores for ion transport, high-power rechargeable batteries can be constructed at the expense of energy density [1-6]. Consequently, many applications were adversely affected by the significant decrease in energy density. This is well recognized for applications requiring high energy density, such as automotive and portable power [7,8]. For more than a century, alkaline batteries have played a significant part in the span of electrical energy batteries systems. As a result, many newly developed energy systems have made alkaline rechargeable systems more suitable for the marketplace. This is mostly sufficient for the vast electronic gadgets market that new and emerging technologies have impacted for many years. The mindset seems to be very different from many other markets [9]. Zinc batteries, which are commonly used for cellular and auditory equipment, have the highest available energy density for the primary battery systems.

Furthermore, these batteries' safety, balanced discharge voltage, and extended life characteristics make them stand out. In addition to its minimal cost, it is regarded as ecologically sustainable compared to other battery systems. It also plays a significant role across a wide range of temperatures [10].

According to the research, the primary disadvantage of zinc-air batteries is their short charge-discharge cycle life owing to the anode (zinc) breakdown and KOH carbonated production. Zinc's high activity can cause it to corrode rapidly in an aqueous medium [11]. Additionally, the primary causes of these batteries' short cycle life have been discovered in other circumstances, including shape change, zinc passivation, and hydrogen evolution (HER) [12].

Due to their high energy density, rechargeable alkali metal-air batteries are regarded the most viable alternative for the power source of electric vehicles (EVs). The practical application of metal-air batteries, on the other hand, remains a challenge.

Many approaches have been devised and tested in the last decade to enhance the development of metal-air batteries. The reaction mechanisms have been steadily understood, and catalysts for air cathodes have been sensibly devised.

* Corresponding author E-mail: hoda_diab2009@yahoo.com, dr_mahmoudelrouby@hotmail.com

Using the charge-discharge technique, the influence of indium and antimony alloying with zinc on the dissolution of a zinc anode and the stability of ZnO film generated at the Zn surface in 6 M KOH solution (the solution used in zinc alkaline batteries) was investigated in this work.

Several synthetic electrodes based on pure zinc with tiny portions of an element as additives can be utilized to achieve those characteristics. Indium was used in very few investigations to slow hydrogen gas generation in KOH solutions, lowering the corrosion rate [13].

This study shows how small alloying metals like indium and antimony can improve discharge time and capacitance when combined with zinc. The purpose is to see how indium and antimony affect charge-discharge processes as well as alkaline battery life. The charge-discharge performance of the two alloys was compared to that of pure zinc in a 6 M KOH solution. This investigation used charge-discharge measurements. Before and after each test, the generated alloys were examined using X-ray diffraction (XRD) and scanning electron microscopy (SEM) (SEM). The investigation outcomes were discussed and compared to data on pure zinc. El-Sayed et al., on the other hand, demonstrated that when Zn is mixed with 0.5-1 percent Sb, its corrosion resistance skyrockets (the corrosion protection efficiency reaches 98.5 percent with the addition of 1 percent Sb) [14, 15].

## 2 Experimental

### 2. 1. Chemicals and Materials

By dissolving a specific amount of potassium hydroxide, a solution of 6 M KOH has been obtained (BDH). Zn-1 % In solid solution and Zn-1 % Sb alloy as electrode materials (disk, A=0.196 $cm^2$) were prepared in an electric furnace using closed and evacuated silica tubes at temperatures of 500 °C and 750 °C of both Zn-1 % In and Zn-1 % Sb alloys, respectively, for one day at a temperature of 500 °C and 750 °C of both Zn-1 % In and Zn-1 % Sb alloys (24 hrs). To maintain the molten homogenous, the melts were agitated every 6 hours. Then, as previously described [16], the mixed melt was allowed to cool by soaking in ice. The alloys Zn-1 percent In and Zn-1 percent Sb were created.

### 2.2. Characterization

The phases of the produced electrodes were determined using Brucker's AXS-D8 advance diffractometer and the Cu-K (=1.5418) detector. A JEOL-5300 mark scanning electron microscope was used to investigate the morphology of the working electrode surface.

### 2. 3. Electrochemical experiments

All electrochemical experiments were achieved in a Pyrex glass cell provided with three electrodes utilizing a Versa STAT4 Potentiostat / Galvanostat. A description of the cell can be found elsewhere [17]. As a working electrode, disk electrodes (Zn, Zn-1 percent In, and Zn-1 percent Sb) inserted in an Araldite holder were used in the electrochemical studies. Before being slotted into the electrochemical cell, the working electrodes were lightly polished with emery paper (1000-1200 m), rinsed with high purity ethanol, and washed in flowing doubly distilled water. A platinum sheet counter electrode was used, and a saturated calomel was used as a reference electrode against which all electrochemical experiment potentials were evaluated.

A continuous voltage of -2.0 V vs. SCE for five minutes in a solution of potassium hydroxide should be applied to clean the surface of the working electrode from any grease and produce oxides. The electrode was then turned off and vigorously agitated to eliminate the adsorbed hydrogen bubbles.

### 2. 4. Charge-discharge technique

Charge-discharge studies were carried out using a potential limited at -1.4 V and -0.9 V and a constant charge-discharge current of 40, 50, 60, 70, 80, and 90 mA.

## 3 Results and discussion

### 3.1. Charge-discharge Technique

In 6 M KOH, without any additives, galvanostatic charge-discharge curves for zinc, Zn-1%In bimetallic, and Zn-1%Sb alloy electrodes are presented in Figure 1. (a, b, c). With increasing current density from -40 to -90 mA, potentials move toward a positive scan, as seen in the figures. The electrodes under research have good discharge performance and decent discharge plateau at various applied current densities. For Zn and its alloys, charge-discharge curves show that the potential shifts toward the negative as the applied current increases. In the case of zinc and alloys, the discharge time decreases as the applied current density increases. It has been discovered that when the current density rises, the capacitance rises.

At an applied current of 40 mA, Figure 2 shows the charge-discharge curves for Zn, Zn-1%In, and Zn-1% Sb electrodes. When comparing the discharging current density and time of zinc and other alloys, it can be noted that Zn-1 % In alloy has the maximum discharging current density and time. This is because the active surface area will be increased due to the presence of indium, as evidenced by SEM pictures (Figure 5). This may be returned to that the radius of the In atom is bigger than the radius of the Zn atom. Furthermore, In has a higher potential for hydrogen evolution than Zn. As shown in equation (1), the specific capacitance can be calculated:

$$S.C = I\,(A) \times t\,(s)/m\,(g) \times \Delta V\ (V) \qquad (1)$$

where S.C is specific capacitance in F/g, where $I$ is the applied current density in Ampere, $t$ time in seconds, m mass of the active species in grams, and $\Delta V$ the potential difference in volts.

Figure 3 depicts the long-term discharge voltage curves of Zn and Zn-In alloys, as well as the capacitance at various current densities. The discharge time of the Zn-1 % In alloy is longer than that of the Zn-1 % Sb alloy and pure Zn, showing that its impedance behavior is better [**18**, **19**]. The average discharge potential difference of Zn-1 % In alloy is -0.78 V, which is larger than Zn-1 % Sb (-0.35V) and Zn-1 percent In alloy (-0.35V) (-0.63 V). These experimental results show that a 1% In alloying with Zn improves energy efficiency compared to a 1% Sb alloying.

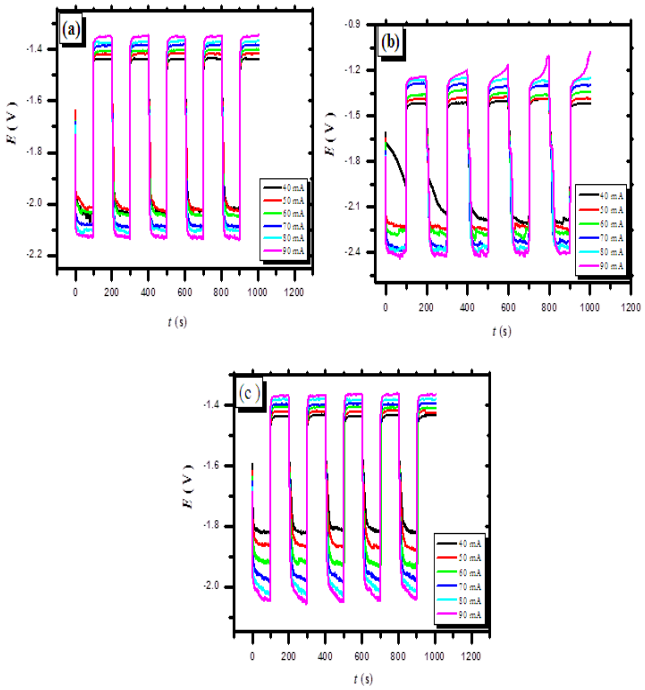


**Fig. 1:** Charge-discharge of Zn (a), Zn 1% In (b), and Zn-1% Sb (c) at different current densities at 25 $^{o}$C.

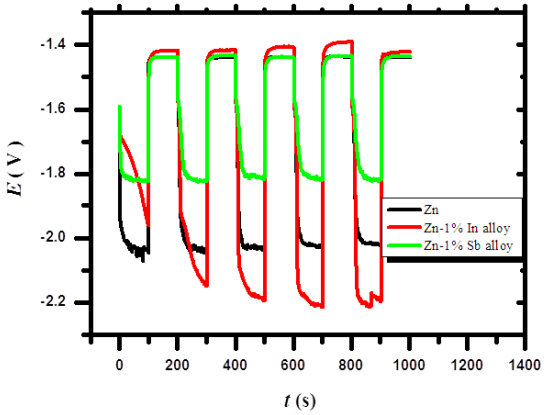


**Fig. 2:** Charge-discharge of Zn, Zn-1%In, and Zn-1%Sb alloys at applied current density 40 mA (a).

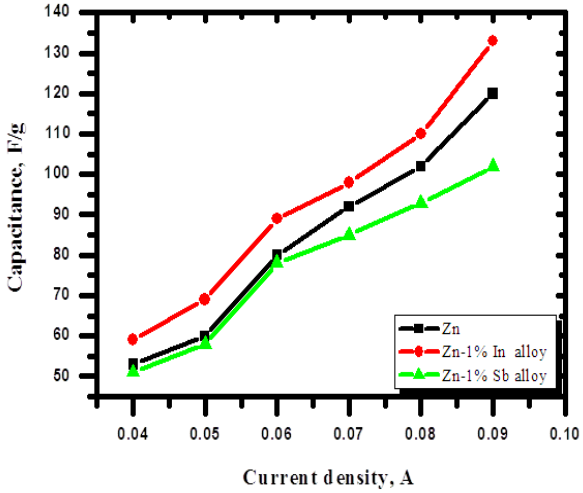


**Fig. 3:** Discharge of the Zn and its alloys at different current densities.

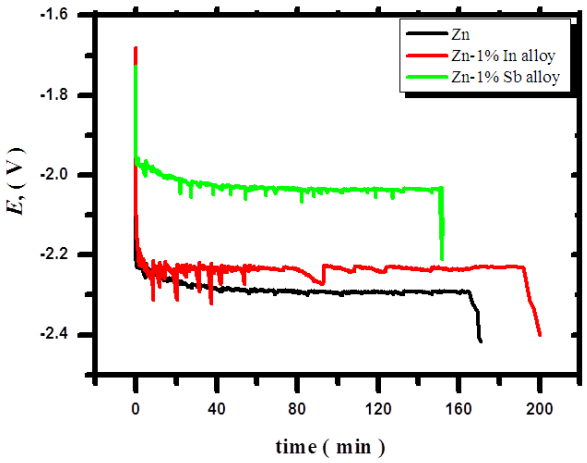


**Fig. 4:** The capacitance at different current densities of Zn and its alloys.

**Table 1:** Capacitance values for pure Zn, Zn-1%In, and Zn-1%Sb electrodes at an applied current density of -40 mA.

| Electrode type / Applied current density (A) | Specific capacity (F/g) | | |
|---|---|---|---|
| | **Zn** | **Zn- 1% In** | **Zn-1% Sb** |
| -0.04 | 174 | 179 | 162 |

This is due to the improvement of the good ion/electron conductivity. As shown in Figure 4 and recorded in Table 1, the discharge curves were used to calculate capacities at a current density of -40 mA. This result shows that the specific capacity of the produced Zn-1 percent In alloy as an electrode steadily rose with indium content compared to the Zn-1 % Sb alloy. Finally, the results reveal that small indium alloying with zinc significantly impacts the alloying of zinc anode batteries in an alkaline medium. The potential of an open circuit is changed to a more negative value for the synthesized Zn-1

% In alloy as an electrode, which accounts for this improvement. As a result, the Zn-1 % In electrode in the 6 M KOH solution employed in the alkaline battery had a longer discharge duration and higher capacitance than the Zn-1 % Sb and pure zinc electrodes.

SEM scans of the oxide film generated at Zinc and Zn-1%In are shown in Figure 5 (a, b). At a magnifying of x500, in electrodes in a solution of 6 M KOH at 25 $^{o}$C in the active region. It's worth noting that the oxide layer created on the alloy surface in the active area appears to be denser and covers almost the entire surface compared to pure Zn. In Figure 5, the produced ZnO looks to be spider-line-like. In the case of alloy I, the generated ZnO oxide is significantly reduced, and another oxide ($In_2O_3$) appears (Zn-1 % In) Figure 4b. The produced $In_2O_3$ prefers big sticks. It coats the whole surface of alloy I. As a result of the SEM pictures, it can be deduced that the presence of indium in the solid solution of Zn-1 percent In alloy provides higher shielding due to the production of its oxide ($In_2O_3$).

At a zoom of 500 times, Figure 5c shows the SEM image of the corrosion layer developed at Zn-1% Sb alloy in 6 M KOH solution at the active region (after corrosion). The corrosion product particles generated on the surface of alloy II are shown in Fig. 5c (Zn-1 % Sb). Some surface components may be visible as a result, and the particles that form on the alloy II surface become stickier and finer. Furthermore, the alloy II micrographs reveal that decreased corrosion product generation on the surface leads to a significant reduction in dendritic growth, resulting in increased corrosion resistance [**13**,**14**, **20**].

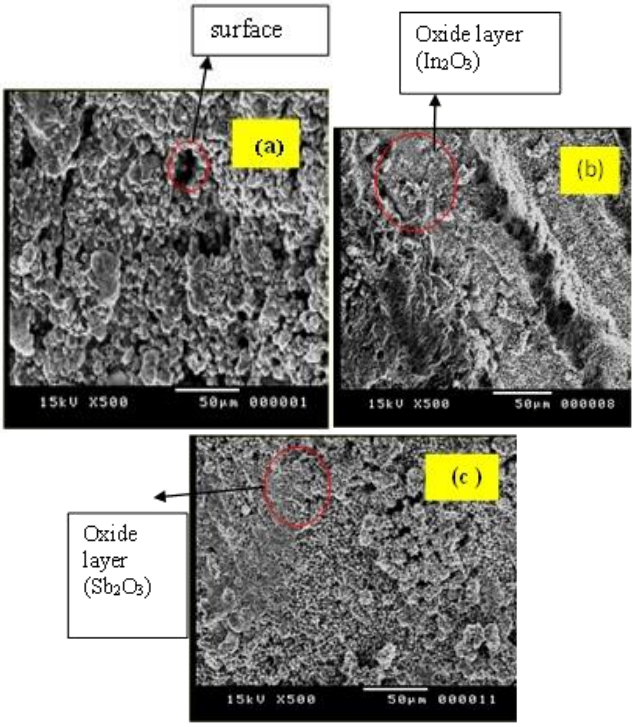


**Fig. 5:** SEM Images layers formed on Zn (a), Zn-1% In alloy (b), and Zn-1% Sb (c) surface at the active region.

Several differences may be detected in Figures 6(a, b, and c) when examining the XRD data. The peaks for Zn and $Zn(OH)_2$ are seen in Figure 6 a. Figure 6b, on the other hand, shows indium peaks with high intensity (at the active region). Both ZnO and $In_2O_3$ have high-intensity peaks in the Xrd spectra of alloy I (as seen in Figure 6 b). This demonstrated that the active portion of the Zn-1 % In alloy surface was coated with both ZnO and $In_2O_3$. In addition to ZnO and $Zn(OH)_2$, the indium oxide on the surface of alloy I is high, and the majority of the surface is virtually coated by this oxide, according to the XRD and SEM data. As a result, all peaks of indium and indium oxides in XRD patterns with high intensities are visible. This suggests that in a Zn-1 percent In alloy, the inclusion of 1% In accelerated the creation of both $In_2O_3$ and ZnO.

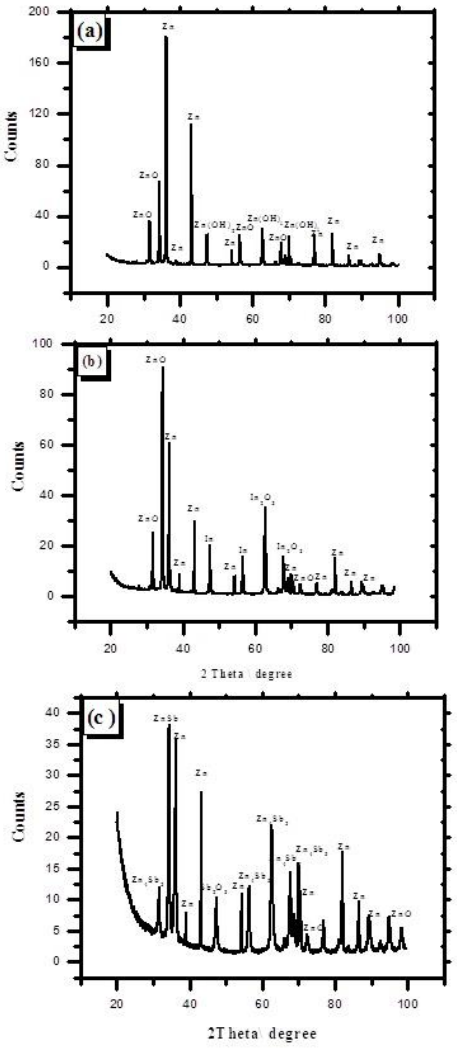


**Fig. 6:** Patterns of X-ray diffraction for the electrochemically formed oxide layers on Zn (a) and the synthesized Zn-1%In (b) and Zn-1%Sb (c) at the active region.

The ZnSb and $Zn_4Sb_3$ phases developed and displayed in the curves in the XRD results of alloy II (Zn-1 percent Sb alloy), as illustrated in Fig. 6c. Furthermore, a peak for $Sb_2O_3$ appears to be near the site of Sb metal. It's worth

noting that the oxides in the alloy's surface layer have a higher intensity than zinc oxides. This demonstrates the formation of ZnO and $Sb_2O_3$ oxides on the alloy surface. This result indicates that the oxides scatter and cover most of the surface of an alloy other than zinc, providing better protection and corrosion resistance.

## 4 Conclusions

The effects of indium and antimony on the electrochemical and corrosion behavior of zinc, as well as its appropriateness for use in alkaline batteries, are the subject of this research.

The discharge time of Zn-1 percent In and Zn-1 percent Sb alloys is compared to their capacitance. Charge-discharge techniques were used in the experiment. Some of the major discoveries are as follows:

1. Charge-discharge experiments show that the potential shifts to a more negative value when the current density increases and the discharge duration increases. Indium alloying increases capacitance. Even so, compared to pure Zn, alloying with Sb reduces capacitance and reduces discharge time.
2. XRD and SEM examinations show that the indium content in the alloy catalyzes the synthesis of ZnO and $Zn(OH)_2$ in an alkaline solution.

With the addition of both In and Sb to Zn, the data obtained (XRD and SEM) of corrosion products generated on the surfaces of the electrodes revealed that $Zn(OH)_2$ is completely gone. On the surface of a Zn-1 % Sb alloy, however, $Sb_2O_3$ has generated additional ZnO.

Also, the newly developed alloys can be considered a good anode for alkaline battery application due to their larger negative open circuit potential, longer discharge duration, and higher capacitance produced than zinc.

## 5 References

[1] Khalifa, H., El-Safty, A., Reda, A., Shenashen, M. A., Slim, M. M., Elmarakbi, A., Metawa, H. A., Theoretical and experimental sets of choice of choice anode/cathode architectonics for high-performance full-scale LIB built-up models, Nano-Micro Letters, 11 (2019) 84.

[2] Khalifa, H., El-Safty, S.A., Reda, A., Shenashen, M. A., Selim, M. M., Alothman, O.Y., Ohashi, N., Meso/macroscopically multifunctional surface interfaces, ridges, and vortex-modified anode/cathode cuticles as force has driven 14701 (modulation of high- energy density of LIB electric vehicles, Sci..Rep.9 (2019) 14701.

[3] Hassen, D. , Shenashen, M. A., El-Safty, A.R., Elmarakbi, A., El-Safty, S. A., Anisotropic N-Graphene –diffused Co3O4 nanocrystals with dense upper-zone top-on-plane exposure facets effective ORR electrocatalysis, Sci. Rep., 8 (2018) 3740.

[4] Shenashen, M. A., Hassen, D., Isago, H., Elmarakbi, A., Hitoshi, Y., Axilly oriented tubercle vien and x-crossed sheet of N-Co3O4 @C hierarchical mesoarchitectures as potential heterogeneous catalysts for methanol oxidation reaction, Chem. Eng. J. 313 (2017) 83-98.

[5] Khalifa, H., El-Safty, S. A., Reda, A., Elmarakbi, A., Shenashen, M. A., Multifaceted geometric 3D mesopolytope cathodes and its directional transport gates for superscalable LIB models, Appl. Mat. Today, 19 (2020) 100590.

[6] Khalifa, H., El-Safty, S. A., Reda, A., Shenashen, M. A., Elmarakbi, A., Metawa, H. A., Structurally folded curvature surface models of geodes/agate rosettes (cathode/anode) as vehicles/truck storage for high energy density lithium ion batteries, Batteries & Supercaps, 3 (2020) 76-92.

[7] Tuck, C.D.S. (Ed.), Modern Battery Technology, EillsHorrwood, New York, 1991.

[8] Berndt, D., Maintenance Free Batteries, Research Studies Press, Taunton, UK., 1997.

[9] VartaBatteric, A.G., Sealed Nickel Cadmium Batteries, VDI Verlag, Duesseldorf, 1982.

[10] Linden, D., Reddy, T.B., Handbook of Batteries,Chapter 13, 3rd ed., McGraw-Hill, 2002

[11] Amin, M. A., Hassan, H. H., Abd El Rehim, S. S., On the role of NO2- ions in passivity breakdown of zinc in de-aerated neutral sodium nitrite solutions and the effect of some inorganic inhibitors using potentiodynamic polarization, cyclic voltammety, SEM and EDX studies, Electrochim. Acta, 53 (2008) 2600-2609.

[12] Frackowiak, E., Skowronski, J.M., Passivation of zinc in alkaline solution effected by chromates and CrO3–graphite system, J. Power Sources 73 (1998) 175-181.

[13] Elrouby,M., Shilkamy, H.A. S., Elsayed, A., Development of the electrochemical performance of zinc via alloying with indium as anode for alkaline batteries application, Journal of Alloys and Compounds, 854 (2021) 157285

[14] El-Sayed, A.R., Shilkamy, H.A.S. Elrouby, M., Tracing the influence of small additions of antimony to zinc on the hydrogen evolution and anodic dissolution processes of zinc as anodes for alkaline batteries application, International journal of Hydrogen energy 46(2021) 31239-31252

[15] El-Sayed, A., Mohran, H.S., Abd El Lateef, H.M., Corrosion Study of Zinc, Nickel, and Zinc-Nickel Alloys in Alkaline Solutions by Tafel Plot and Impedance Techniques, Metall. Mater. Trans. A 43 (2012) 619-632.

[16] Abd El-Rehim, S.S., Hassan, H.H., Mohamed, N.F., Anodic behavior of tin in maleic acid solution and the effect of some inorganic inhibitors, Corros. Sci. 46(2004)1071–1082.

[17] El-Sayed, A., Shaker, A.M., Abd El-Lateef, H.M.,: Corrosion inhibition of tin, indium and tin–indium alloys by adenine or adenosine in hydrochloric acid solution, Corros. Sci. 52(2010) 72–81.

[18] Ding, Y., Wen, C., Hodgsona, P., Li, Y., Effects of alloying elements on the corrosion behavior and biocompatibility of biodegradable magnesium alloys: a review, J. Mater. Chem. B 2 (2014) 1912–1933.

[19] Zhang, Y., Lia, Q., Guoa, T., Li, S., Effect of Y Content on Properties of Extruded Zn-1.5Mg-xY Alloys for Medical Applications, Mater. Res. 22 (Suppl. 2) (2019) 20190004.

[20] El-sayed A, Mohran HS, Abd El-Lateef HM. Effect of minor nickel alloying with zinc on the electroche- -mical and corrosion behavior of zinc in alkaline solution. *J Power Sources* 195(2010)6924-36.